A novel single-polarization single-mode photonic crystal fiber with circular and elliptical air-holes arrays*

LI Xin (黎昕)[1]**, **ZHENG Hong-jun** (郑宏军)[1,2,3], **WU Chong-qing** (吴重庆)[2], **and LIU Shan-liang** (刘山亮)[1]

1. School of Physics Science and Information Technology, Liaocheng University, Liaocheng 252059, China

2. Key Laboratory of Luminescence and Optical Information, Ministry of Education of China, School of Science, Beijing Jiaotong University, Beijing 100044, China

3. State Key Laboratory of Advanced Optical Communication Systems and Networks, Shanghai Jiao Tong University, Shanghai 200240, China

(Received 29 September 2012)

A novel single-polarization single-mode photonic crystal fiber (SPSM-PCF) with circular and elliptical air-holes is proposed. The characteristics of the proposed SPSM-PCF are investigated by using a full-vector finite element method (FEM) with perfect matched layer (PML) boundary conditions. The results show that the SPSM operation is achieved with wider band, and the total dispersion profile of the SPSM-PCF is dispersion-flattened from 1.193 μm to 1.384 μm. This dispersion property makes the proposed SPSM-PCF useful for various applications, such as optical transmission and dispersion compensation for conventional fiber at long wavelength band with 500 nm negative dispersion region. It indicates that this is a good solution to realize broadband SPSM operation.

Document code: A **Article ID:** 1673-1905(2013)02-0120-4

DOI 10.1007/s11801-013-2365-3

Since the first photonic crystal fiber (PCF) was demonstrated by Russell[1], PCFs with design flexibility and incomparable advantages have been attracting much attention and are extensively investigated[1-3]. PCFs can achieve single-polarization single-mode (SPSM) operation by designing proper PCF structure. The SPSM-PCFs can be applied in high power fiber lasers, sensing and optical communication systems, because it can eliminate both polarization mode coupling and polarization mode dispersion. Some groups have studied PCFs for SPSM operation[4-11]. The PCFs perform the SPSM operation with bandwidth of 55 nm in the 1550 nm band[4], 220 nm in the 727 nm band[5], 84.7 nm and 103.5 nm in the 1300 nm and 1550 nm band[6], 460 nm[7], 560 nm[8], 250 nm[9], 120 nm[10], and 600 nm[11], respectively. In this paper, we propose a novel SPSM-PCF with circular and elliptical air-holes in order to achieve dispersion-flattened profile, wider bandwidth and negative dispersion for SPSM operation. The characteristics of proposed SPSM-PCF are investigated by using the full-vector finite element method (FEM) with perfect matched layer (PML) boundary conditions.

Fig.1 shows the cross-section of the proposed SPSM-PCF. The inner cladding of proposed PSM-PCF is square lattice of circular air-holes, and the outer layer is composed of three-rings hexagonal lattice of elliptical air-holes. The proposed PCF can perform SPSM operation because of the three-rings hexagonal lattice of elliptical air-holes. The low dispersion is induced by the square lattice of circular air-holes.

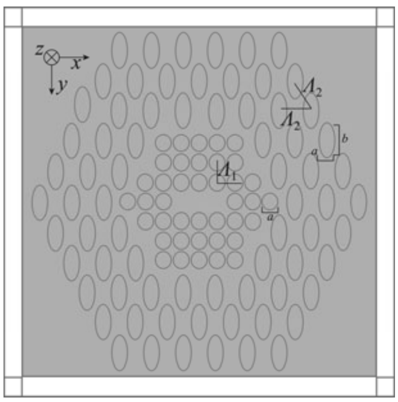

Fig.1 Cross-section of the proposed SPSM-PCF

The gray area denotes pure silica, the elliptical and circular areas represent air holes, and the rectangular

* This work has been supported by the National Natural Science Foundation of China (Nos.60778017 and 61077048), the Beijing Municipal Natural Science Foundation (No.4092031), the Shandong Provincial Natural Science Foundation (No.ZR2011FM015), the State Key Laboratory of Advanced Optical Communication Systems and Networks, Shanghai Jiao Tong University (No.2011GZKF031101), the Shandong Provincial Young Core Instructor and Domestic Visitor Foundation for University Key Teacher, and the Research Foundation of Liaocheng University in China.

** E-mail: lixin1@lcu.edu.cn

areas at the edges represent PML boundary. The diameter of circular air holes is a=0.45 μm, and the spacing between the circular air holes is Λ_1=1.00 μm. The diameters of the elliptical air holes along the x-axis and y-axis are denoted as a and b, respectively. The spacing between the elliptical air holes is Λ_2=1.80 μm, and the elliptical ratio is $\eta=b/a$=2, where a=0.45 μm, and b=2a =0.90 μm. The refractive indices of the silica regions and the air holes are 1.45 and 1, respectively. The mode field characteristics can be modified by the shape and the spatial distribution of these air holes.

The Helmholtz equation can be obtained from Maxwell equations[10, 11]

$$\nabla\times([\mu_r]^{-1}\nabla\times\boldsymbol{E})-k_0^2[\varepsilon_r]\boldsymbol{E}=0\,, \quad (1)$$

where $k_0=2\pi/\lambda$ is the free-space wave number, λ is the wavelength of input light, $\boldsymbol{E}=E(x,y)^{j\beta z}$ denotes the electric field, β is propagation coefficient, $[\varepsilon_r]$ and $[\mu_r]$ are the relative dielectric permittivity and magnetic permeability tensors, respectively. According to the full-vector FEM, we can obtain complex effective index n_{eff} from the eigenvalue equation of Eq.(1). The model birefringence B of the proposed SPSM fiber is given by the difference between the effective indices of two orthogonal polarization modes[11-13], and the beat length of model birefringence is defined by $L_B=\lambda/B$.

The confinement loss of the SPSM-PCF is defined by[11-14]

$$\alpha_{dB}=1000\times40\pi\times\mathrm{Im}(n_{eff})\,/(\mathrm{In}(10)\cdot\lambda)\quad(\mathrm{dB/km})\,, \quad (2)$$

where Im(n_{eff}) is the imaginary part of the effective index n_{eff}. The dispersion, which is an important parameter of the fiber, includes the material dispersion and waveguide dispersion. The material dispersion can be obtained from the Sellmeier equation[11-15]

$$n^2=1+\sum_{j=1}^{m}\frac{B_j\cdot\lambda^2}{\lambda^2-\lambda_j^2}\,, \quad (3)$$

and group-velocity dispersion parameter equation [11-15]

$$D=-\frac{\lambda}{c}\cdot\frac{\mathrm{d}^2n}{\mathrm{d}\lambda^2}\,, \quad (4)$$

where n is the refractive index of the medium, λ is the input optical wavelength, m=3, B_1=0.6961663, B_2=0.4079426, B_3=0.8974794, λ_1=0.0684043 μm, λ_2=0.1162414 μm, λ_3= 9.8961610 μm, and $\lambda_j=2\pi c/\omega_j$, where ω_j is the medium resonance radian frequency, and c is the speed of light in vacuum. The group-velocity dispersion parameter D is useful in practice. The waveguide dispersion is obtained from Eq.(4) and the variation of the real part of effective index n_{eff} with the wavelength. The complex effective index and modal field distribution can be obtained from solving Eq.(1) by using the full-vector FEM. The confinement loss and dispersion can be obtained from Eq.(3) and (4), respectively.

We firstly calculate the confinement losses of a PCF with three-ring arrays of circular air holes by our full-vector FEM with PML boundary conditions. The calculation is well consistent with that of Ref.[16].

The electric field distributions of x-polarized and y-polarized fundamental modes of the proposed SPSM-PCF at the wavelength of 1.550 μm are shown in Fig.2. The horizontal arrow denotes x-polarized mode, and vertical one shows y-polarized mode. It can be obtained from Fig.2 that the mode fields of x- and y-polarized modes are basically symmetrical about x- and y-axes. The electric field of y-polarized mode is more obviously extended to the cladding region than that of x-polarized one. The y-polarized confinement loss is much larger than that of x-polarized mode.

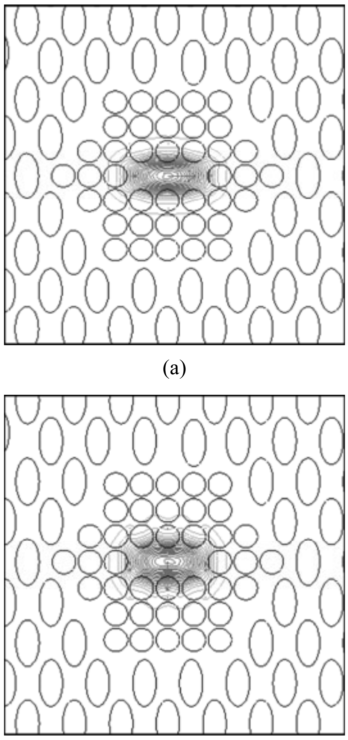

(a)

(b)

Fig. 2 Electric field distributions of (a) *x*-polarized and (b) *y*-polarized modes of the proposed SPSM-PCF at the wavelength of 1.550 μm

The modal birefringence is 1.458×10^{-2}, and the beat length is 0.106 mm at the wavelength of 1.550 μm. The confinement losses of x- and y-polarized modes are 3.100×10^{-4} dB/km and 1.721 dB/km, respectively. It is assumed that the transmission span is 80 km, and transmitter power is 0 dBm according to general optical communication systems. After propagation over 80 km of the proposed SPSM-PCF, the powers of x- and y-polarized modes are reduced to -2.480×10^{-3} dBm and -1.377×10^{2} dBm, respectively. The experimental noise of a good detector (e.g. optical spectrum analyser AQ6319) is about -60 dBm. It shows that y-polarized mode is suppressed, and x-polarized mode can be detected and amplified in the systems. Thus, the SPSM operation is achieved by using the proposed PCF. The SPSM-PCF can be extensively applied in the field devices. The numerical aperture of the x-polarized mode is 0.447, the effective mode area is 3.066 μm^2, and the nonlinear coefficient is 34.373 $W^{-1}\cdot km^{-1}$ at the wavelength of 1.550

μm.

Fig.3 shows the effective index and the modal birefringence varying with input wavelength. It is obtained from Fig.3 that the effective indices of *x*- and *y*-polarized modes are increased with the decrease of the wavelength. The effective index of *x*-polarized mode increases from 1.284 to 1.413 with the decrease of the wavelength. The effective index of *y*-polarized mode decreases from 1.409 to1.256 with the increase of the wavelength. The effective index of *y*-polarized mode is smaller than that of *x*-polarized mode for a given input wavelength. The modal birefringence of the proposed SPSM-PCF is almost linearly increased with the increase of the wavelength.

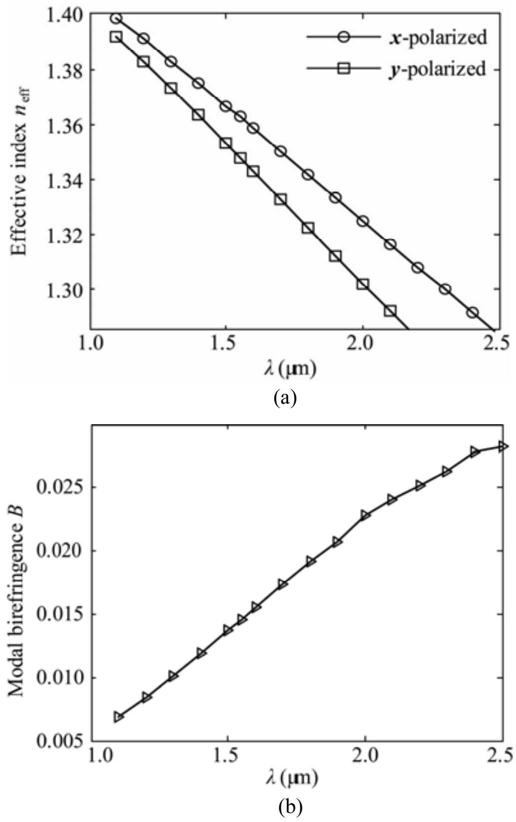

Fig.3 Variations of (a) effective indices and (b) modal birefringence with input wavelength

Variations of confinement loss and confinement loss difference between *y*-polarized mode and *x*-polarized one with input wavelength are shown in Fig.4. The confinement losses of *x*- and *y*-polarized fundamental modes are almost exponentially increased with the increase of the input wavelength. The confinement loss of *x*-polarized mode is increased from 3.854×10^{-7} dB/km to 1.757×10^{4} dB/km with the increase of the input wavelength. That of *y*-polarized one is increased from 8.951×10^{-7} dB/km to 1.806×10^{7} dB/km. The confinement loss of *y*-polarized mode is much larger than that of *x*-polarized mode for a given input wavelength. The confinement loss difference between the *y*-polarized fundamental mode and the *x*-polarized one is rapidly increased approximately exponentially from 1.100 μm to 2.000 μm. The confinement loss difference is increased from 5.097×10^{-7} dB/km at the wavelength of 1.100 μm to 1.804×10^{7} dB/km at the wavelength of 2.500 μm. It shows that the confinement loss is increased with the increase of input wavelength. The diffraction effect of air holes is enhanced with the increase of input wavelength, while the effect of air holes for blocking the light into the cladding is weakened. According to the discussion on SPSM operation above, the PCF can perform SPSM operation with input wavelength from 1.550 μm to 2.500 μm.

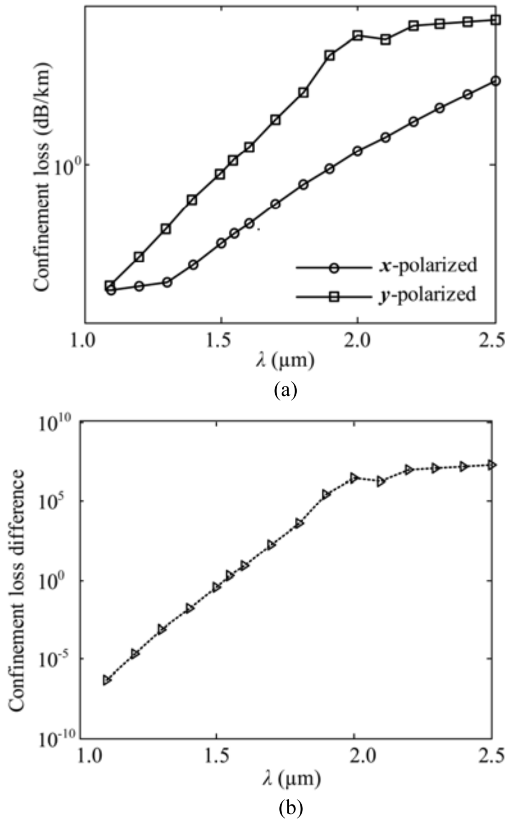

Fig.4 Variations of (a) confinement loss and (b) the difference with input wavelength

Variations of the dispersion with input wavelength are illustrated in Fig.5. The dispersion flattened characteristic of optical communication systems is a hot spot. The material dispersion is gradually increased with the increase of wavelength. The waveguide dispersion is decreased with the increase of wavelength from 1.100 μm to 2.500 μm. It results in that the total dispersion profile is convex and dispersion-flattened from 1.193 μm to 1.384 μm. The dispersion parameters of the proposed PCF are 83.482 ps/(km·nm) at the wavelength of 1.193 μm and 83.480 ps/(km·nm) at the wavelength of 1.384 μm, and the maximum dispersion parameter is 85.477 ps/(km·nm) at the wavelength of 1.286 μm. The dispersion flatness of the proposed SPSM-PCF, which means subtracting minimum parameter from the maximum parameter in the range of the wavelength, is 2.039 ps/(km·nm). It is much better than the flatness 9.000 ps/

(km·nm) from 0.830 μm to 1.020 μm[17], and is slightly less than the flatness 1.800 ps/(km·nm) from 1.480 μm to 1.620 μm[18]. The dispersion flattened region of the proposed SPSM-PCF is 191 nm, which is almost equal to the width of 190 nm in Ref.[17], and wider than the bandwidth of 140 nm in Ref.[18] and the width of 100 nm in Ref.[19]. This dispersion property makes the proposed SPSM-PCF useful for various applications. The total dispersion value is negative from 2.015 μm to 2.500 μm. The dispersion is -125.142 ps/(km·nm) at the wavelength of 2.500 μm. It shows that the PCF can be applied in dispersion compensation for conventional fiber in optical communication systems.

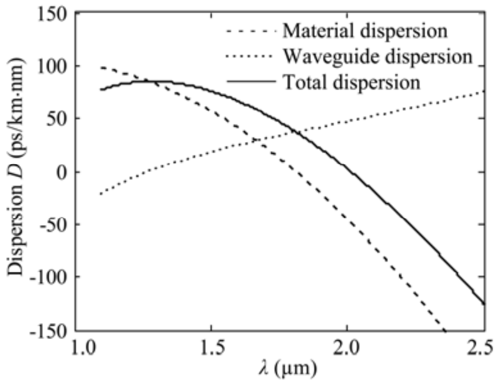

Fig.5 Variations of dispersion with input wavelength

The modal birefringence is 1.458×10^{-2}, and the beat length is 0.106 mm at the wavelength of 1.550 μm. The confinement losses of *x*- and *y*-polarized modes are 3.100×10^{-4} dB/km and 1.721 dB/km, respectively. The proposed PCF can perform SPSM operation because of the suppression of *y*-polarized mode. The SPSM operation is achieved with wider band of 950 nm. The total dispersion profile of the SPSM-PCF is dispersion-flattened from 1.193 μm to 1.384 μm. This dispersion property makes the proposed SPSM- PCF useful for various applications. The SPSM-PCF can be applied in dispersion compensation of conventional fiber at long wavelength band with 500 nm negative dispersion region.

References

[1] J. C. Knight, T. A. Birks, P. St. J. Russell and D. M. Atkin, Opt. Lett. **21**, 1547 (1996).

[2] J. C. Knight, J. Broeng, T. A. Birks and P. St. J. Russell, Science **282**, 1476 (1998).

[3] P. St. J. Russell, Science **299**, 358 (2003).

[4] Daniel A. Nolan, George E. Berkey, Ming-Jun Li, Xin Chen, William A. Wood and Luis A. Zenteno, Opt. Lett. **29**, 1855 (2004).

[5] J. R. Folkenberg, M. D. Nielsen and C. Jakobsen, Opt. Lett. **30**, 1446 (2005).

[6] Jian Ju, Wei Jin and M. Suleyman Demokan, J. Lightw. Technol. **24**, 825 (2006).

[7] Fangdi Zhang, Min Zhang, Xiaoyi Liu and Peida Ye, J. Lightw. Technol. **25**, 1184 (2007).

[8] Ming-Yang Chen, Bing Sun and Yong-Kang Zhang, J. Lightw. Technol. **28**, 1443 (2010).

[9] Dora Juan Juan Hu, Ping Shum, Chao Lu, Xia Yu, Guanghui Wang and Guobin Ren, Appl. Opt. **48**, 4038 (2009).

[10] Kunimasa Saitoh and Masanori Koshiba, IEEE Photonics Technology Letters **15**, 1384 (2003).

[11] Hongjun Zheng, Chongqing Wu, Shanliang Liu, Huishan Yu, Xin Li, Zhen Tian and Weitao Wang, Optical Engineering **50**, 125003 (2011).

[12] Lin An, Zheng Zheng, Zheng Li, Tao Zhou and Jiangtao Cheng, J. Lightw. Technol. **27**, 3175 (2009).

[13] Tzong-Jer Yang, Lin-Fang Shen, Yuan-Fong Chau, Ming-Je Sung, Daru Chen and Din Ping Tsai, Optics Communications **281**, 4334 (2008).

[14] Ming-Yang Chen, Rong-Jin Yu and An-Ping Zhao, J. Lightw. Technol. **23**, 2707 (2005).

[15] G. P. Agrawal, Nonlinear Fiber Optics, Singapore: Elsevier Pte Ltd., 1 (2009).

[16] Masanori Koshiba and Kunimasa Saitoh, IEEE Photonics Technol. Lett. **15**, 691 (2003).

[17] WANG Wei, LIU Zhao-lun, HAN Ying and HOU Lan-tian, Optoelectronics Letters **8**, 363 (2012).

[18] LI Xin, ZHENG Hong-jun, YU Hui-shan and LIU Shan-Liang, Optoelectronics Letters **8**, 48 (2012).

[19] T. Yamamoto, H. Kubota, S. Kawanishi, M. Tanaka and S. Yamaguchi, Opt. Express **11**, 1537 (2003).